JOURNAL OF CATALYSIS 157, 244–258 (1995)

Proton Affinity Distributions of TiO_2–SiO_2 and ZrO_2–SiO_2 Mixed Oxides and Their Relationship to Catalyst Activities for 1-Butene Isomerization

Cristian Contescu,*,[1] Vlad T. Popa,*,[1] James B. Miller,† Edmond I. Ko,† and James A. Schwarz*,[2]

*Department of Chemical Engineering and Materials Science, Syracuse University, Syracuse, New York 13244-1190; and
†Department of Chemical Engineering, Carnegie Mellon University, Pittsburgh, Pennsylvania 15213-3890

Received March 28, 1995; revised July 10, 1995; accepted July 18, 1995

Proton-releasing properties at the oxide/aqueous solution interface were examined as a function of pH for two series of mixed oxide aerogels and their pure oxide components using potentiometric titrimetry. Reports of synthesis, surface characterization, and catalytic activity (1-butene isomerization) have appeared recently for similar preparation batches of titania–silica and zirconia–silica. After deconvolution of potentiometric titration data, the pK spectra of the oxide surfaces were obtained; they reveal the number and strength of various proton donor sites present under "wet" conditions. The activity in 1-butene isomerization measures weak Brønsted sites of the "pseudo-dry" catalyst (reaction at 423 K after drying at 473 K). We find that the activity for 1-butene isomerization is linearly related to the density of a *particular type* of proton donor site determined from pK spectra. This shows that only a limited number of the total Brønsted sites accessed by potentiometric titrimetry is specifically active for 1-butene isomerization under the conditions used here. The pK range of active sites and the corresponding TOF numbers are $6.3 < pK < 8.7$, $(8.2 \pm 2.1) \times 10^{-3}$ s^{-1} for titania–silica and $6.4 < pK < 6.5$, $(93 \pm 24) \times 10^{-3}$ s^{-1} for zirconia–silica. In the two catalysts series the catalytic performance varied with either composition (titania–silica) or preparation parameters (zirconia–silica) at constant composition. © 1995 Academic Press, Inc.

INTRODUCTION

Insight into acidic/basic properties of solid catalysts (in terms of both abundance and strength) may be obtained by combining characterization techniques with test reactions. Several characterization techniques are currently used for probing surface acid sites but their results often face the difficulty of separating the contribution of Brønsted and Lewis acidity. Total acidity (Lewis and Brønsted) is usually obtained either from TPD of ammonia or other selected bases or from amine titration with Hammett color indicators. However, when these methods are used to characterize the acid strength distribution, the information obtained should be cautiously considered and regarded on a relative scale. The reason is that, regardless of other experimental details that may influence the results (equilibration times, particle size), the *state of the surface* during the acidity measurements can often be very different from that of the catalyst under reaction conditions. For example, in the TPD method acid strengths are compared in terms of desorption temperatures; titration with Hammett indicators is carried out under *nonaqueous* conditions, but one compares the sample's ability to protonate various basic indicators that differ by their p*K* in *aqueous* media.

FT–IR is more specific in probing surface hydroxyls (either isolated or perturbed by adsorbed H bond acceptors) and demonstrates how different they are in terms of acid–base properties. As a complementary method, adsorption of molecular probes reveals sites available for either proton transfer or coordinative bonding and is largely used to distinguish between Brønsted and Lewis acidity. However, the knowledge of surface density of Brønsted sites (*absolute numbers*) is often needed in catalytic studies for evaluation of specific reaction rates of acid-catalyzed reactions. In this respect, the Brønsted to Lewis *ratio* determined by spectroscopic means (pyridine adsorption) is not sufficient, since the total number of (potential) acidic sites has still to be measured by another method (such as ammonia TPD) under different experimental conditions.

Using a catalytic reaction as a measure for "catalytic acidity," although more pragmatic, was more successful and led to important findings. Cracking and skeletal isomerization of alkanes demands strong Brønsted sites; double-bond isomerization is one of the least demanding reactions in terms of the strength required for active sites (1). Recently, attention was focused on several classes of mixed

[1] Permanent address: Institute of Physical Chemistry of Romanian Academy, Spl. Independentei 202, Bucharest 77208, Romania.
[2] To whom correspondence should be addressed.

0021-9517/95 $12.00

oxide systems that show increased acidity and enhanced catalytic activity in comparison with the pure components. Since their properties depend on both the composition and the degree of homogeneity, several strategies for a better control of the preparation methods were investigated.

Titania–silica displays unique properties for acid-catalyzed reactions, such as butene isomerization (2–5), ethene hydration (6), isopropanol dehydration (7), and cumene dealkylation (7), in contrast to the parent pure oxides. In these reactions, the activity was linked to the Brønsted acidity (2–5) and especially to the *weak* Brønsted sites (8).

Zirconia–silica is another system studied for its catalytic significance (9, 10). Recently its activity in acid-catalyzed reactions [isomerization of 1-butene (11), dehydration of cyclohexanol (12) and of isopropanol (13)] was studied in combination with other methods for surface characterization (14) with the goal to design strategies for better control of catalyst microstructure during preparation steps (11, 15).

Although it was evident that the preparation techniques affected both the physical properties and "catalytic acidity," the evaluation of strength and abundance of those Brønsted sites that are specifically active on the catalyst surface was not straightforward. Miller *et al.* (5) used FT–IR of adsorbed pyridine to determine the *fractional* content of Brønsted sites on titania–silica, but they needed an independent estimation of the *total* number of acidic sites. Bosman *et al.* (12) found a quasi-linear correlation between areal rates for cyclohexanol dehydration on zirconia–silica and the acid site concentration from ammonia TPD, but they also showed the existence of some acid sites on pure silica and pure zirconia that do not contribute to the alcohol dehydration. On titania–silica, Liu *et al.* (4) tried to avoid the ambiguities associated with using ammonia TPD as a diagnostic of acidity and performed, instead, a version of a TPD experiment in the IR spectrometer whereby the contribution from Brønsted and Lewis sites could be separated. They also used adsorption of 2-propanol and temperature-programmed dehydration of 2-propanol as a more specific probe for those surface Brønsted sites that contributed to the increased activity for 1-butene isomerization observed for titania-rich mixed oxides. The presence of strong Lewis sites, which were also reported (16) to be active for 1-butene isomerization, could be ruled out based on the *cis-trans*-product isomer ratio that serves as a diagnostic for the reaction mechanism.

Recently there has been an increased interest in the characterization, prediction, and modeling of proton-binding properties of surface hydroxyls at the oxide–solution interface (17–20). Collectively, the results have shown that proton-binding–proton-releasing equilibria at the oxide–solution interface are determined by intrinsic crystallochemical properties. In other words, the proton affinity of oxygen or hydroxyl sites at the oxide–solution interface is determined by the same factors (number and type of subadjacent coordinated metal ions) that are responsible for the differences in acid–base properties of the corresponding Brønsted sites on "dry" (or "pseudo-dry") surfaces of the same oxides.

We reported previously (20–23) a method for characterizing proton-binding properties at the solid–solution interface of various solid samples [oxides (20–24), activated carbons (25)] in terms of a proton affinity distribution (PAD) or pK spectrum. The method allows for a quantitative characterization of the "wet" interface with respect to both the number (surface density) and the strength (apparent pK values) of surface groups involved in binding or releasing protons. In several instances we proposed that the features shown by the pK spectra could be assigned to oxo- or hydroxo-groups with different local coordination at the oxide–solution interface (20–23, 26).

Here we report the use of proton affinity distributions determined from potentiometric titration as a means to obtain reliable quantitative information on the Brønsted acidity of mixed oxidic systems. In particular, with the availability of catalytic data, a linear relationship was found between the surface density of surface sites of a particular acid strength at the hydrated oxide surface and the specific catalytic activity for 1-butene isomerization of the same samples.

EXPERIMENTAL

Materials

We studied two series of mixed oxide aerogels prepared by Miller *et al.* (5, 15). For the sake of comparison we also characterized the pure oxide phases. Table 1 lists the physical parameters of all samples.

All titania–silica samples (TS-*X* series) used here were from preparation batches similar to the prehydrolyzed titania–silica aerogels described recently by Miller *et al.* (5). Details on their preparation can be found in the original paper. The independent variable in this series is the SiO_2 content (X) of the aerogels, which took the values 5, 33, 50, and 67 mol%.

In the zirconia–silica series (ZS-PHR samples) the molar ratio of the components was kept constant (1 : 1) and the conditions of the synthesis method were carefully controlled. The independent variable for this series is the water to silicon molecular ratio (prehydrolysis ratio, PHR), a parameter systematically varied during preparation to promote better mixing of the components and improve the homogeneity of the mixed oxide. The preparation method was documented by Miller *et al.* (11); we used the same samples as those described in Ref. (15).

Two titania polymorphs (anatase and rutile) were obtained from Aldrich. The nominal phase purity in each sample is greater than 99.9%. Pure silica xerogel was made in our laboratory by slowly hydrolyzing a tetraethylor-

TABLE 1

Characteristics of Reference Oxides and Catalysts Samples

	Independent Variable	BET area ($m^2 g^{-1}$)	Isomerization activity (mmol $m^{-2} h^{-1}$)	Brønsted sites fraction (%)
		A. Pure Oxides		
Rutile	none	8	n/a	-
Anatase	none	40	n/a	-
Silica	none	425	n/a	-
Zirconia	none	89	none	-
		B. Titania–silica catalysts[a]		
	% SiO_2	BET area	Isomerization activity	Brønsted sites fraction
TS-5	5	215	0.018	6
TS-33	33	318	0.064	26
TS-50	50	375	0.048	32
TS-67	67	405	0.037	32
		C. Zirconia–silica catalysts		
	PH ratio	BET area	Isomerization activity	Brønsted sites fraction
ZS-0	0	244	0.094	29
ZS-0.65	0.65	262	0.097	26
ZS-1.13	1.13	268	0.105	33
ZS-2.68	2.68	186	0.118	38
ZS-3.22	3.22	186	0.135	39

[a] The activity and fractional Brønsted acidity data are for the samples originally reported in Ref. (5); BET data are for a second batch of identically prepared samples.

thosilicate (Aldrich)—ethanol (Aldrich)—deionized water emulsion at 323 K. After drying at 383 K for 20 h, the gel was calcined at 873 K for 6 h. Pure zirconia aerogel was prepared by a procedure similar to that used for the zirconia–silica samples (27).

Methods

The procedure used for potentiometric titration was documented previously and the errors affecting the results were discussed (20, 22, 23). All data were collected under a protective nitrogen atmosphere by using a combination glass electrode (Accu-pHast) and an Accumet-50 pH/mV-meter (Fisher Scientific). A Metrohm 665 Dosimat was used for the delivery of the titrant (0.1 *N* certified volumetric solution of NaOH, from Aldrich) and the corresponding pH data were continuously recorded by a computer which was interfaced with the pH meter.

All 1-butene isomerization activity tests were done according to a procedure described by Miller *et al.* (5). After drying the samples in helium at 473 K for 1 h, the temperature was reduced to 423 K and the gas feed changed to the reaction mixture (5% 1-butene in He). Activity is reported as the isomerization rate on a per area basis, after 95 min time on stream.

Calculations

We have previously documented the calculation method by which the pK spectra of the oxide–solution interface were obtained. It comprises several calculation steps:

1. Transforming the titration curve (pH vs volume of titrant) into a proton-binding curve (millimoles of protons adsorbed or released by the solid sample as a function of solution pH) and its recalculation on an area basis. We used BET surface areas measured by the standard procedure with N_2.
2. Smoothing the experimental errors by using cubic splines. An objective criterion was used for the smoothing (20) which ensured that all significant information was retained and random errors were minimized.
3. Deconvoluting the proton-binding curve

$$\Theta([H]) = \int_{\log K_{min}}^{\log K_{max}} \theta(K, [H]) F(\log K) d(\log K) \qquad [1]$$

and calculating the proton affinity distribution from the integral equation for proton adsorption. A truncated approximation of *r*th order calculated by the local solution method for the integral equation is

$$F_r(\log K) = \sum_{n=0}^{n=r} \left[\frac{(-1)^n \pi^{2n}}{\ln(10)^{2n+1}(2n+1)!} \left(\frac{\partial^{2n+1}\Theta(\log [H])}{\partial(\log [H])^{2n+1}} \right)_{\log[H] = -\log K} \right]. \qquad [2]$$

We used the so-called RJ approximation which corresponds to $r = 1$. Here K is the local equilibrium constant for proton binding to the surface where the local coverage, $\theta(K, [H])$, is described by a Langmuir-type isotherm. Denoting by K_a the proton release constant of the corresponding hydroxyls (with the same local coordination), the relationship between the proton affinity constant from equations (1) and (2) and the (classical) acidity constant is $pK_a = \log K$.

The approach assumed above, in which the oxide surface is described as a collection of *different, but not interacting* acid–base sites is, in fact, equivalent to the more conventional picture of the oxide–solution interface, in which one considers the existence of *identical, but interacting* surface hydroxyls (28). We chose the former picture because an apparent pK spectrum is readily available from experimental data. Also, in the present approach we avoid the uncer-

tainty related to the choice of parameters needed for modeling the electrostatic interaction between charged groups.

4. Correcting for the buffering effect of water. By definition, the buffer intensity (or buffer index) of a system represents the tendency of that system to resist a pH change upon addition of strong base (or strong acid). At any point of a titration curve, the buffer intensity (β) is inversely proportional to the slope of the titration curve. For a solution of monoprotic acid with concentration C, a simple calculation (29) gives

$$\beta = \frac{d\,C_B}{d\,(\mathrm{pH})} = -\frac{d\,C_A}{d\,(\mathrm{pH})} = 2.3\{C\alpha_A\alpha_{HA} + [H^+] + [OH^-]\} \quad [3]$$

where C_B (or C_A) is the concentration of strong base (or strong acid) added as titrant(s) and α_A and α_{HA} are the degree of protolysis and the degree of formation, respectively, of the weak acid HA. Buffer intensity is at maximum (titration curve has a distinct inflection) at the equivalence point where $\alpha_A = \alpha_{HA}$ or $[HA] = [A^-]$ and $pH = pK_a$. This enables quantitative use of acid–base titrimetry.

Aqueous solutions are strongly buffered at both ends of the pH scale, where either the $[H^+]$ or the $[OH^-]$ term of the above relationship dominates. The neutral and quasi-neutral pH range defines a practical pH window where the titration curve is sensitive to the intrinsic properties of the (weak) acids or bases in the titration mixture.

5. Analyzing the resulting affinity spectrum both qualitatively (identifying the occurrence of different categories of surface Brønsted sites) and quantitatively (estimating their contribution to the total proton-binding curve). We previously tried different methods of decomposing an affinity spectrum of simple model compounds to find a convenient way for quantitative analysis of various sites. The result of the RJ approximation was in excellent agreement with the assumed distribution when the latter was Gaussian, in contrast with the result calculated for a delta Dirac distribution of log K values (20). We therefore chose to decompose the affinity spectrum with Gaussian functions. A similar approach, which made use of Gaussian-like distributions, was reported by Rudzinski *et al.* (30, 31) for the analysis of multicomponent ion adsorption on alumina, titania, and other oxide materials. Multi-Gaussian distributions with different numbers and heights of the peaks were also used by Jagiello (32) to represent distributions with a certain diversity of shapes.

For Gaussian fitting we used the Peakfit software (Jandel Scientific) and the quality of the fit was judged from the values of the standard deviation and correlation coefficient. As an additional constraint, we preferred fits with the minimum possible number of components and rejected those fits where the Gaussian half-width exceeded 0.8 pK values.

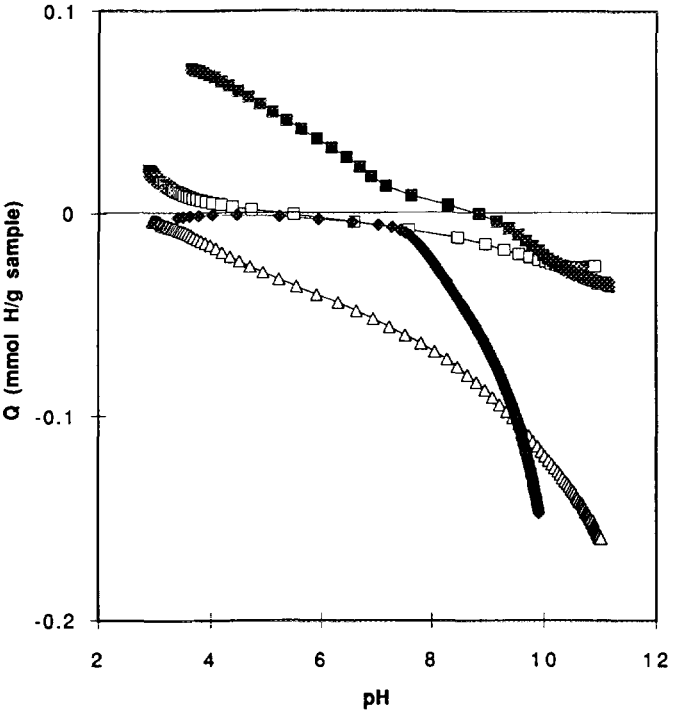

FIG. 1. Proton-binding isotherms for pure oxides. The data for silica were scaled by a 0.1 factor. (□) Rutile, (△) anatase, (◆) silica, (■) zirconia.

The later limit was found from separate experiments with simple model compounds, as described elsewhere (20, 25). The results obtained were not significantly different when other distributions (such as log-normal) were tried.

RESULTS AND DISCUSSION

Corrections at the End of the pH Scale

The proton-binding curves calculated from potentiometric titration data are shown in Figs. 1–3. Since positive values for Q (pH) indicate proton uptake and negative values show proton release, the crossover point is a measure of acidity or basicity. Silica and anatase are acidic, rutile is amphoteric, zirconia is rather basic; all other samples show to a greater or lesser extent Brønsted acidity under the conditions used in their characterization.

Figure 4 illustrates the perturbation due to the "buffering power of water" (29). In Fig. 4a, the PADs calculated for a series of model solutions of sodium acetate (pK_a = 4.75) of known concentrations are compared, on a concentration scale, with the PAD obtained from a blank titration experiment and the theoretical buffer index of water given by

$$\beta_{water} = \frac{d\,C_B}{d\,\mathrm{pH}} = -\frac{d\,C_A}{d\,\mathrm{pH}} = 2.3\,([H^+] + [OH^-]). \quad [4]$$

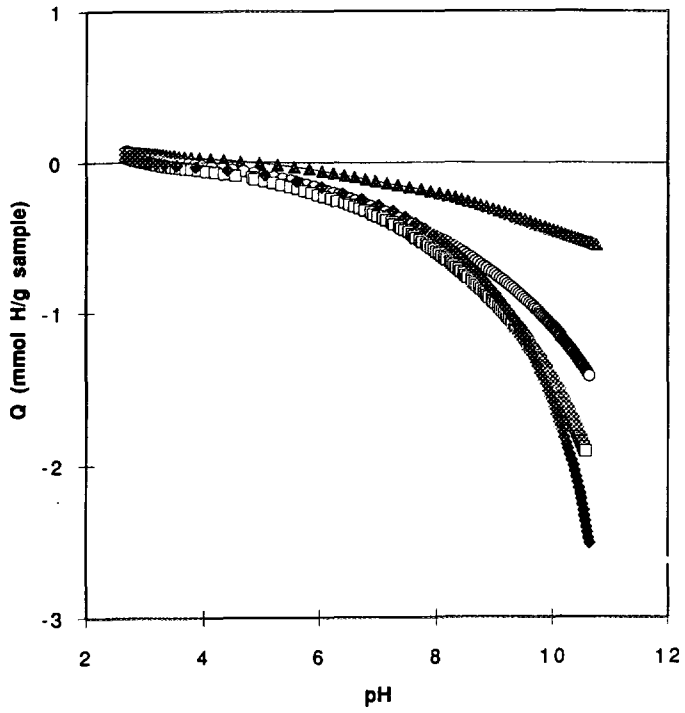

FIG. 2. Proton-binding isotherms for titania–silica (TS) samples. The independent variable is SiO_2 content (mol%) in aerogels. Details on preparation in Ref. (5). (▲) TS-5, (○) TS-33, (□) TS-50, (◆) TS-67.

In Fig. 4b the pK spectra of several solid samples used in this study are compared, on the same concentration scale, with β_{water}. For the sake of comparison, all pK spectra shown in Fig. 4 were calculated with $r = 0$ in Eq. (2), which corresponds to the condensation approximation (CA) (20).

It is seen that at both ends of the pH scale, where either the $[H^+]$ or the $[OH^-]$ term of the above relationship dominates, aqueous solutions are strongly buffered. With the classical calculation procedures it was estimated (33) that acids or bases weaker than pK $\approx$ 9 cannot be titrated in water; or in other words, the pH window extends from pH 5 to 9. In our experiments we were able to obtain accurate titration data within the pH interval from 3 to 11; outside this range, slight deviations occurred between the calculated and experimental blanks which became important for pH < 2 and pH > 12.

The pH window whereby meaningful proton affinity spectra may be obtained from experiment depends on the sample and experimental conditions. In all cases where the concentration of free H^+ or OH^- exceeds that of H^+ or OH^- consumed by the titrated sample, spurious "wings" result in the calculated pK spectra. In Fig. 4a they are seen at pH < 4 and pH > 10 for sodium acetate solutions. However, the higher the concentration of sodium acetate solutions, the better resolved from the "water background" is the corresponding PAD. When the PADs calculated from experimental data at the extreme pH range were corrected by subtracting β_{water}, the results were, for all concentrations, a quasi-symmetrical distribution curve centered correctly at the position of pK_a for acetic acid. The broadness of the distribution is a result of the mathematical approximations used. In separate experiments with homogeneous solutions we used Gaussian fitting of resulting distributions to retrieve the amount of titrated compounds in a variety of solvents (34).

For solid samples, Fig. 4b shows that the perturbation due to water depends on pH and sample. For a sample with low surface area (rutile, 8 m^2 g^{-1}) the window of reliable information extends from pH 4 to 10 whereas this range extends to pH $\approx$ 11 for samples with high surface area such as titania–silica and zirconia–silica. However, even for the latter samples, the details seen in the distribution at the low pH extreme (pH < 4) should be disregarded because they fall outside the confidence range. In other words, as expected, silica and its congeners do not have surface groups able to react with protons in the acidic range. Spurious "wings" are also shown by the PAD of TS-5 sample at pH > 11 (low concentration of surface groups) but are not characteristic of ZS samples at the same pH. In addition, an abrupt increase in the buffer

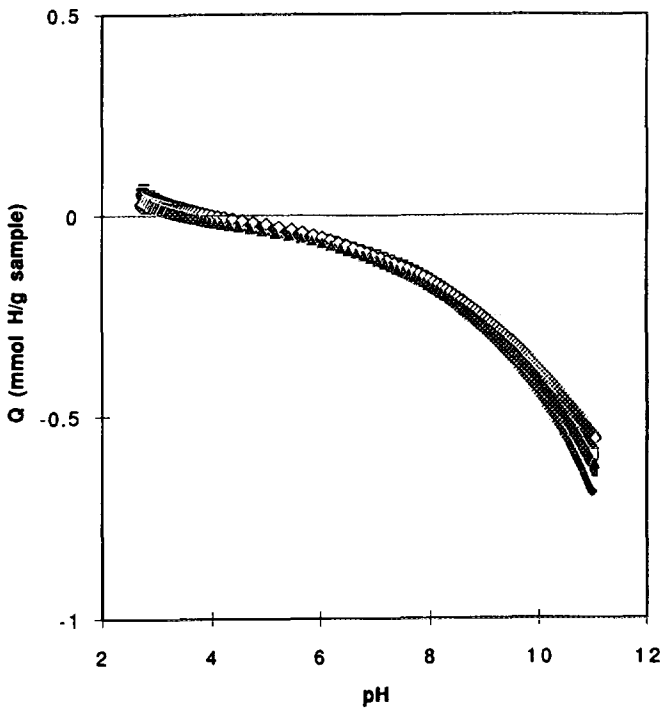

FIG. 3. Proton-binding isotherms for zirconia–silica (ZS) samples. The independent variable is the prehydrolysis ratio (PHR) during the preparation step. Details on preparation in Ref. (15). (■) ZS-0. (□) ZS-0.65, (◆) ZS-1.13, (◇) ZS-2.68, (▲) ZS-3.22.

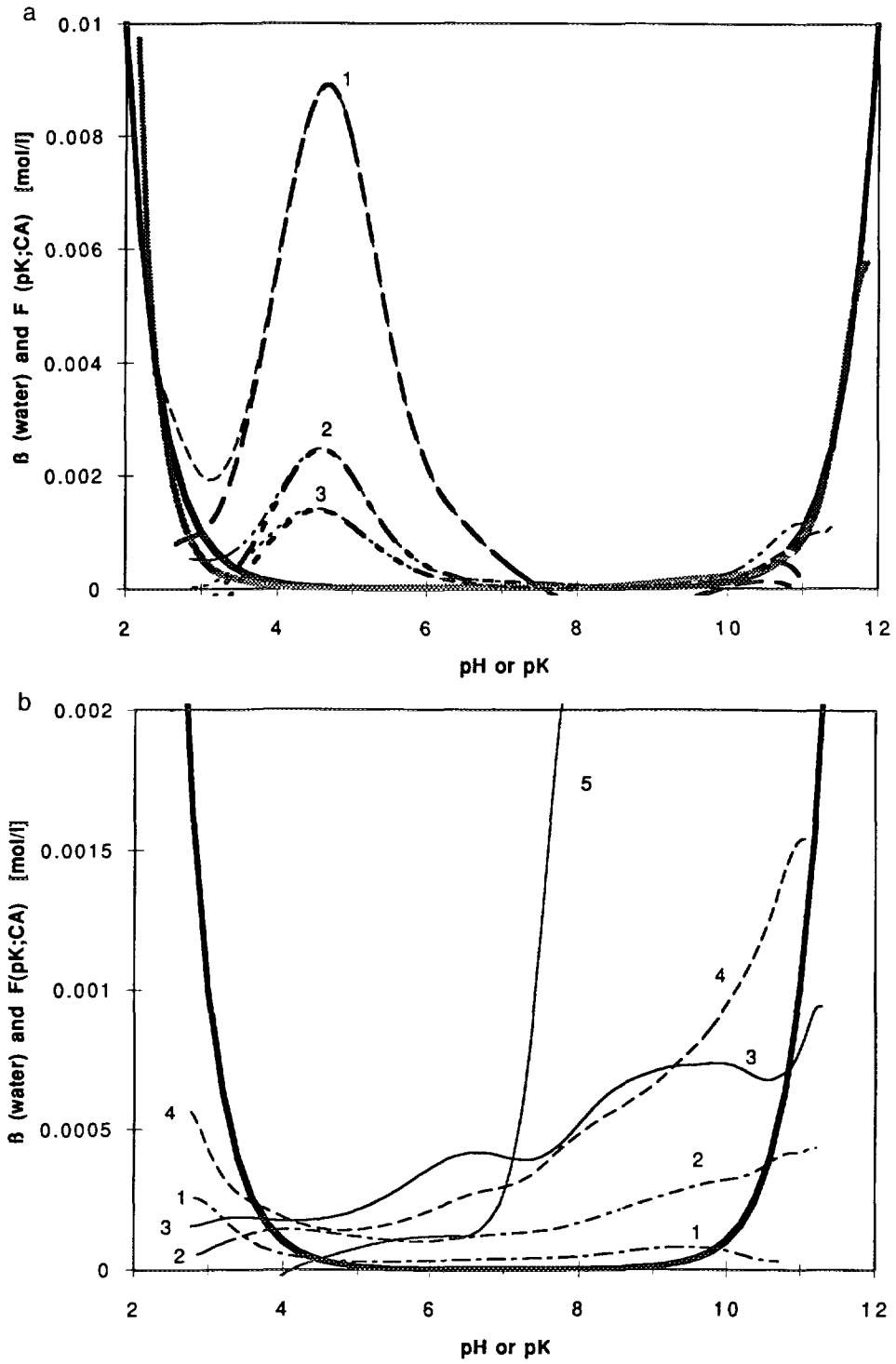

FIG. 4. The experimental pH window determined by the buffering effect of water at both ends of the pH scale depends on the concentration of titrable groups offered by the sample. (a) The buffer index for water, β_{water} (solid black line), and the result of a blank experiment (solid grey line) are plotted on the concentration scale and compared with experimental PADs (expressed in mol liter^{-1}) for model sodium acetate solutions of various concentrations: (1) 0.0178 *M*; (2) 0.0047 *M*; (3) 0.0027 *M*. For the same model solutions also shown are PADs corrected by subtracting β_{water}. (b) The buffer index for water β_{water} (solid black line), is plotted together with experimental PADs (expressed in mol liter^{-1}) for selected oxide and catalysts samples at different surface-to-volume ratios during titration: (1) rutile, 80 m^2 liter^{-1}; (2) anatase, 400 m^2 liter^{-1}; (3) TS-5, 1290 m^2 liter^{-1}; (5) silica, 2550 m^2 liter^{-1}.

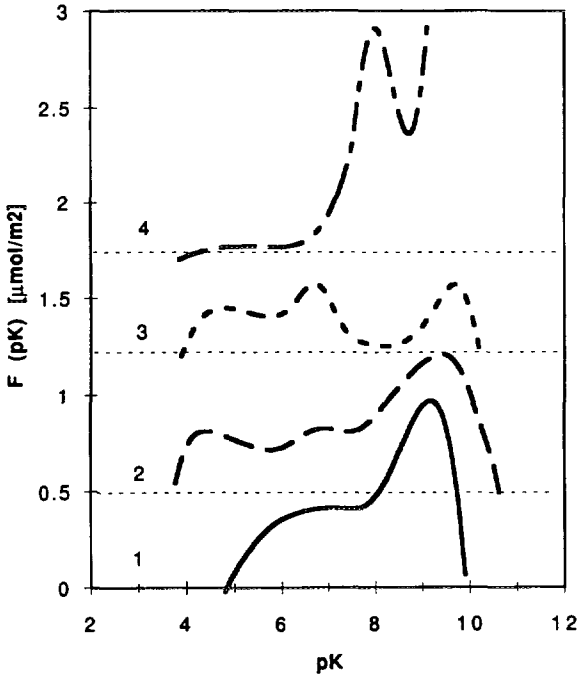

FIG. 5. Proton affinity distributions (corrected for water buffering) of pure oxides: (1) rutile; (2) anatase; (3) zirconia; (4) silica. The zero level of each curve was shifted for clarity, as shown by the dotted lines.

index may reflect the onset of dissolution. This is the case with the silica sample in the extremely basic pH range.

The PADs of pure oxides and the two catalyst series shown in Figs. 5–7 were corrected for the buffering influence of water and the wings at high and low pH were greatly attenuated although not completely removed.

In Fig. 8 we show several examples of Gaussian decomposition for typical samples. At this point we should stress that any fitting procedure implies a set of conventions which should be fully considered in discussion of results. Decomposition of a complex, asymmetric peak of the pK spectrum into a sum of Gaussians may be misleading with regard to the number of component peaks; using asymmetric functions (such as beta distributions) would be more significant (smaller number of components) but at the expense of a more subjective choice of parameters needed to describe asymmetric peaks. We preferred to limit the number of curve-fitting parameters, although, in some instances, this led us to include additional Gaussians on the tail of asymmetric peaks. Our choice for Gaussians is motivated by the need for a flexible and user-friendly instrument for analyzing components of complex profile curves.

The data collected in Table 2 indicate the parameters of Gaussian components found from the fitting and the values of the corresponding correlation coefficients. The most important information in this table is the acid strength (pK_i) and surface density (N_i) of proton binding sites revealed by potentiometric titration.

Relations with Specific Catalytic Activity

Using the results from Table 2, we checked whether or not a correlation could be found between the surface density of Brønsted acid sites revealed by PADs and the catalytic activity for 1-butene isomerization measured for the same samples.

After screening all possible correlations, we have found that, although several surface sites were identified in PADs, *there is only one type of site* for each group of samples whose abundance could be correlated with the areal rates of the catalytic reaction measured under the conditions state (catalyst at 423 K after dehydration at 473 K). As Fig. 9 shows, the specific reaction rate (μmol m^{-2} h^{-1}) increases linearly with the surface density (μmol m^{-2}) of surface sites able to bind or release protons in a narrow pH range. The range is pH 6.3–8.7 for titania–silica and pH 6.4–6.5 for zirconia–silica samples. The correlation coefficients of the linear relationships shown in Fig. 9 equal 0.971 for the former system and 0.913 for the latter. Assuming that the catalytic sites were correctly identified and their surface density under the reaction conditions does not differ much from the result of potentiometric titration, the turnover frequency for butene isomerization could be

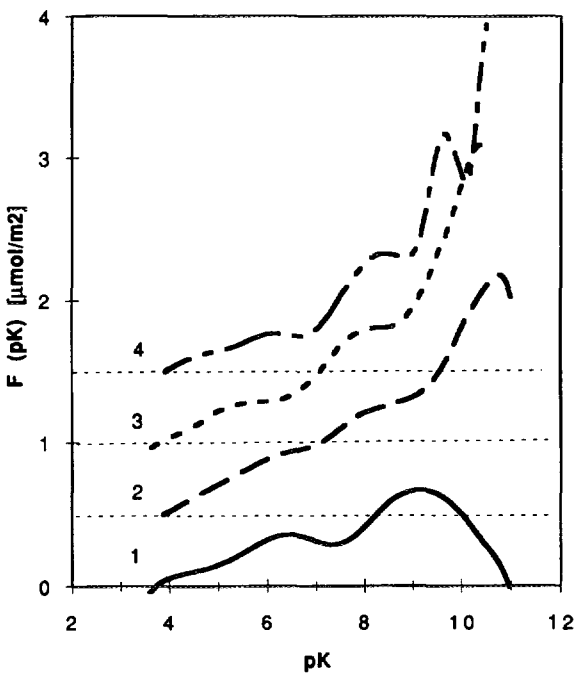

FIG. 6. Proton affinity distributions (corrected for water buffering) of titania–silica samples: (1) TS-5; (2) TS-33; (3) TS-50; (4) TS-67. The zero level of each curve was shifted for clarity, as shown by the dotted lines.

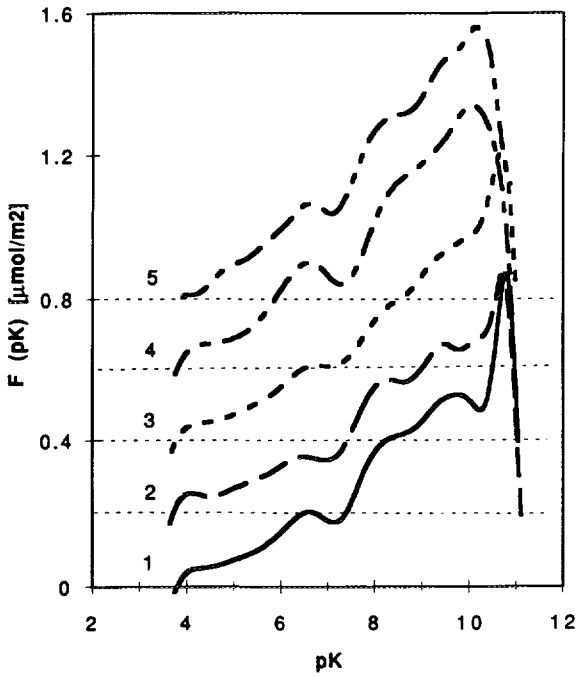

FIG. 7. Proton affinity distributions (corrected for water buffering) of zirconia–silica samples: (1) ZS-0; (2) ZS-0.65; (3) ZS-1.13; (4) ZS-2.68; (5) ZS-3.22. The zero level of each curve was shifted for clarity, as shown by the dotted lines.

calculated. The values are $(8.2 \pm 2.1) \times 10^{-3}$ s^{-1} for silica–titania and $(93 \pm 24) \times 10^{-3}$ s^{-1} for zirconia–silica. For comparison, the slopes of the lines in Fig. 9 are 9.2×10^{-3} s^{-1} and 86×10^{-3} s^{-1}, respectively.

"Wet" versus "Dry" Surface: An Apparent Dichotomy

Almost all oxides are active as catalysts for isomerization of alkenes, which is one of the least demanding reactions in terms of acid strength required (1). However, the activity and selectivity vary among different oxides.

The *cis/trans* ratio is often used as an indication of the mechanism in the case of alkene isomerization by double-bond migration. A ratio near unity shows the involvement of a carbenium ion intermediate formed by proton abstraction from the catalyst; in this case, the activity is a good measure of Brønsted acidity (2). A higher value of the *cis/trans* ratio indicates a mechanism via a carbanion intermediate that was formed on a basic surface site. It is interesting to note that pretreatment conditions may switch the reaction pathway from one mechanism to another. For example, 1-butene isomerization on Cr_2O_3 activated at 570–720 K occurs on acid Brønsted sites (surface hydroxyls); on the same catalyst, after a more severe activation that leaves a dehydroxylated surface (evacuation at 1025 K) isomerization occurs on basic sites (surface oxygens) (35).

Silica was reported to be inactive for butene isomerization (2) although some residual acidity could be found with Hammett indicators (2, 12). Pure titania is known to possess a high concentration of strong Lewis acids and weak Brønsted acidity (16); these properties should be linked to the ease of its dehydroxylation. After activation at 473 K, small, comparable activities were measured for pure titania and the TS-5 sample studied here. With increasing silica content in the TS series the activity reached the highest level for the TS-33 sample and then declined for silica-rich samples. The *cis/trans* ratio was always indicative of the mechanism involving Brønsted sites (5).

Pure zirconia aerogel displays exclusively Lewis acidity and is inactive for 1-butene isomerization (36). Bosman *et al.* (12) reported that incorporating of both Zr in a SiO_2 matrix and Si in a ZrO_2 matrix led to catalysts with higher activity for acid-catalyzed dehydration of cyclohexanol; the optimum activity was found around a 1 : 1 composition. At the same composition, ZS samples reported here (15) and other similarly prepared zirconia–silica aerogels (11) isomerize 1-butene by the mechanism that involves weak Brønsted sites. The fine tuning of catalytic activity acquired by a variation of the prehydrolysis ratio in the sol-gel step and the response of PADs to this variation, illustrated in Fig. 7, are remarkable.

One might question the relevance of the information obtained by potentiometric titration as a measure of Brønsted sites' contribution to catalyst performance since the state of the surface is different under the conditions of catalytic testing (flowing gas feed at 423 K after dehydration at 473 K) and those of potentiometric titration (aqueous electrolyte solution at 298 K). The main differences are (1) the degree of hydration and (2) the temperature. We analyze next their contribution to the results reported.

Role of Surface-Bound Water

The common feature for the catalyst surface both in the wet state (i.e., during potentiometric titration) and the pseudo-dry state (i.e., during activity tests) is the existence of a strongly bound layer of water that completes the coordination of surface cations. In both states, the chemistry within this layer mediates the intensity and direction of proton transfer.

For the wet surface, the proton affinity of surface oxygen sites depends on the number and nature of surrounding metal ions and on the number of hydrogen bonds needed to complete the coordination by elements of water at the surface (19). It is considered that the layer of hydrogen-bonded water molecules is probably confined to one monolayer (37) and the adjacent layers are more or less bulk like (38).

For the pseudo-dry surface, experimental data show that a mild dehydration is required for development of activity

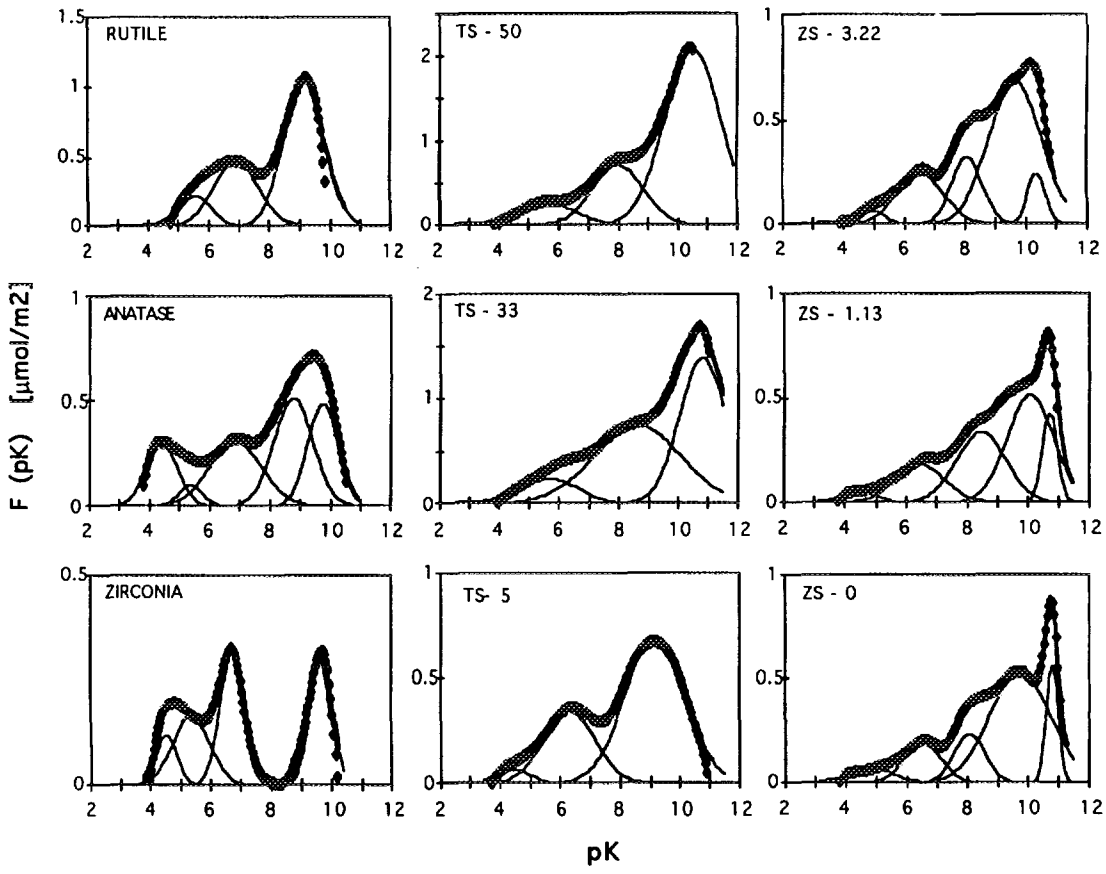

FIG. 8. Selected examples showing the decomposition of calculated PADs (diamonds) into a sum of Gaussians (solid lines).

in reactions catalyzed by weak acids, such as double-bond isomerization of 1-butene. Ko *et al.* (2) have previously shown for coprecipitated titania–silica that too high a dehydroxylation temperature produced catalysts with low activity, whereas addition of water to samples dehydrated at 573 or 773 K restored partially the activity.

Using *in situ* FT–IR spectroscopy, Miller *et al.* (5, 15) characterized the surfaces of ZS and TS samples at conditions chosen to simulate those used in 1-butene isomerization. For both series of samples, the IR spectra in the surface hydroxyl region revealed a large hydroxyl population, perturbed by hydrogen bonding, in addition to isolated silanol groups. In the titania–silica group, the hydrogen-bonded population became more numerous as the silica content increased, again in agreement with the difficulty to dehydroxylate silica compared to titania. For zirconia–silica samples (with constant composition) the hydroxyl population perturbed by hydrogen bonding was constantly large and the silanol vibration diminished as the prehydrolysis ratio increased.

There is experimental evidence that an important hydroxyl population persists on the surface of mildly dehydrated catalysts subjected to reaction tests. Under the reaction conditions used here, the proton abstraction by the 1-butene reactant is probably mediated by hydroxyls of the pseudo-dry catalyst surface. The catalytic activity depends on the number and strength (proton-donating ability) of acidic sites. The identification and characterization of active sites for particular reactions is not straightforward. However, proton release by the wet catalyst surface can be quantified in terms of a pK spectrum from potentiometric titration data. Figure 9 demonstrates that, for 1-butene isomerization, a linear correlation exists between the *concentration of acid sites of a particular strength* (revealed by PADs) and the reaction rate per surface unit (specific activity).

Although a correlation was expected, it was not found before when catalyst acidity was characterized by other methods. For coprecipitated titania–silica, Ko *et al.* (2) observed a larger variation in isomerization activity than in acidity (Benesi titration with *n*-butylamine), which was ascribed to the fact that *n*-butylamine titrates both Brønsted and Lewis acid sites whereas isomerization measures only Brønsted acidity. For the same system and using similar methods, Itoh *et al.* (6) measured a variation in isomerization activity by a factor of 10 while acidity varied by no more

TABLE 2

Results of Gaussian Analysis of Proton Affinity Distributions

	pK	μmol m^{-2}	pK	μmol m^{-2}	pK	μmol m^{-2}	pK	μmol m^{-2}	pK	μmol m^{-2}	pK	μmol m^{-2}	r^2
A. Pure Oxides													
Rutile	—	—	5.6	0.29	6.9	0.89	—	—	9.1	1.72	—	—	0.994
Anatase	4.4	0.39	5.4	0.10	6.9	0.67	8.8	0.82	9.7	0.60	—	—	0.999
Silica	—	—	—	—	—	—	8.0	1.37	9.7	2.78	—	—	0.998
Zirconia	4.5	0.10	5.4	0.26	6.7	0.31	9.6	0.29	—	—	—	—	0.979
B. Titania–silica catalysts													
TS-5	4.5	0.09	—	—	6.3	0.73	—	—	9.2	1.72	—	—	0.993
TS-33	5.7	0.54	—	—	8.6	2.63	—	—	10.8	2.70	—	—	0.999
TS-50	5.7	0.59	—	—	8.0	1.54	—	—	10.5	4.90	—	—	0.999
TS-67	5.8	0.43	—	—	8.2	1.48	—	—	9.7	1.81	10.8[a]	4.31[a]	0.912
C. Zirconia–silica catalysts													
ZS-0	4.9	0.11	—	—	6.5	0.29	8.0	0.29	9.7	1.35	10.8[a]	0.27[a]	0.998
ZS-0.65	4.1	0.03	—	—	6.4	0.39	8.1	0.30	9.5	0.87	10.7[a]	0.37[a]	0.984
ZS-1.13	4.6	0.06	—	—	6.5	0.37	8.5	0.69	10.1	0.98	10.77[a]	0.26[a]	0.999
ZS-2.68	4.7	0.12	—	—	6.5	0.47	8.7	1.11	10.0	0.68	10.6[a]	0.18[a]	0.996
ZS-3.22	4.9	0.06	—	—	6.5	0.48	8.1	0.41	9.7	1.48	10.4[a]	0.17[a]	0.999

[a] Uncertain data at the extreme pH limits.

than twice. For zirconia–silica, Bosman *et al.* (12) showed recently a rather scattered plot of specific rates (area basis) for cyclohexanol conversion versus the acid site concentration (NH_3 retained at 473 K from ammonia TPD).

Effect of Temperature

Proton affinity constants depend on temperature as all free energy functions. Generally, proton adsorption is exothermic. This results in a decrease of apparent pK values with an increase in temperature; the variation may be as high as 1.5–2 pK units for 50 K. For the alumina–water interface we have found that both the enthalpic and entropic terms for proton adsorption depend on the uncompensated local charge of oxygen bonding sites and the enthalpic term is perturbed by electrostatic effects (22).

The results shown in Table 2 correspond to measurements at 298 K. We did not study the temperature variation of apparent pKs for the samples reported here, so that the values that would correspond to the temperature of catalytic tests are unknown. On the basis of previous results with alumina, we may only speculate that all samples would exhibit higher acidic strengths (smaller pK values) at least for several surface groups (several peaks in PADs).

Comparison of PADs with Other Data on Catalyst Acidity

There is still little agreement on the strengths and surface densities of acid sites on mixed oxides. For the system discussed here, acid strength measured with *n*-butylamine titration and Hammett indicators showed sites as strong as $H_0 = -8.2$ for coprecipitated titania–silica (2); $H_0 = -11.4$ for zirconia–silica (12); $H_0 = -5.6$ for precipitated titania (2); $H_0 = +1.5$ for zirconia (12) and an acid strength of $+3.3 < H_0 < +7.1$ for silica (12). These data cannot be compared with the results from PADs, which apparently show a much lower acidity under wet conditions. Recall that although acidity comparisons were facilitated by Hammett's approach, the effect of changing the medium (water for potentiometric titration and the usual pH scale; anhydrous organic solvents for amine titration and the H_0 scale) does complicate any comparison of acidity in a fundamental way (39). The leveling of acidities to the $0 < pK_a < 14$ range caused by water is another practical difference that prohibits comparisons.

In aqueous solutions charged species are stabilized by water dipoles and solvation effects contribute significantly to the values of acidity constants. This is the reason why the acidity scale based on proton affinities in the gas phase, which is free of complicating effects due to solvation, differs from the acidity scale in water. However, the general view (1) supported by experimental proof (40), is that polarizable oxygen ions on oxide surfaces may stabilize the charge of adsorbed molecules as if they were in aqueous solutions. The aqueous solutions acidity scale is therefore more appropriate to compare the relative Brønsted acidity of surface hydroxyls.

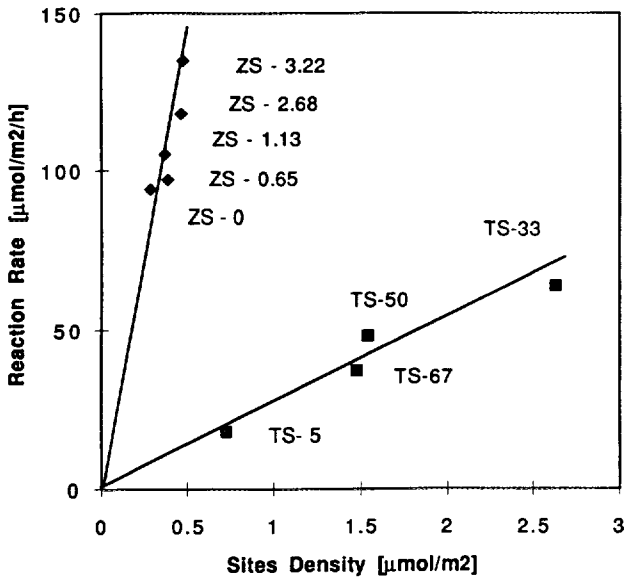

FIG. 9. Linear relationship between specific reaction rates for isomerization of 1-butene (μmol m^{-2} h^{-1}) and surface density of active Brønsted sites (μmol m^{-2}) for TiO_2–SiO_2 catalysts (squares, $6.3 < pK < 8.7$) and ZrO_2–SiO_2 catalysts (diamonds, $6.4 \leq pK < 6.5$) calculated from PADs.

In water, pyridine (pK_a 5.25) is a weaker base than ammonia (pK_a 9.25). All acids stronger than pK 9.25 will protonate ammonia; those stronger than pK 5.25 will protonate both pyridine and ammonia. The relative basicity of these molecules in water should be conserved when they interact with various surface Brønsted acids.

According to the data from Table 2, silica has no acidic sites able to protonate ammonia at 298 K, but all other samples have sites strong enough to form NH_4^+. Sites that could protonate pyridine occur on anatase and, in a limited number, on TS-5. This type of strong site is more abundant on zirconia and ZS samples. We will examine briefly the agreement of that conclusion with other information available in the literature.

There is no general agreement on the definition of strong, weak, hydrogen bonded, and other forms of adsorbed ammonia identified by ammonia-TPD. Results of Bosman *et al.* (12) for zirconia–silica samples have shown that the catalytic activity (cyclohexanol dehydration) could be correlated with the number of strongly bound ammonia molecules (i.e., still adsorbed at 473 K) but the correlation was quite poor. On titania–silica, Liu *et al.* (4) demonstrated by FT–IR and NH_3-TPD that ammonia adsorption occurs on strong Lewis sites (on pure titania) and on quite weak Brønsted sites on other samples. Therefore ammonia-TPD could be used only to measure total acidities.

More precise information came from FT–IR data; this method distinguishes between adsorbed molecules bonded coordinatively on Lewis sites, surface NH_4^+ or PyH^+ ions held by Brønsted sites, and molecules interacting weakly through hydrogen bonds; however, quantification is more difficult.

Depending on the method of preparation, pure titania showed only a limited number of Brønsted sites able to protonate reversibly ammonia (41) or no Brønsted sites at all (42), in addition to a large population of strong Lewis sites and hydrogen bond donors. Precipitated TiO_2–SiO_2 samples were characterized as very weak Brønsted acid solids, which were unable to protonate substantially either pyridine (a weak base), or ammonia and *n*-butylamine (stronger bases) (42). On the contrary, on more homogeneous Ti–Si mixed oxide catalysts, Liu *et al.* (4) observed, by FT–IR, the occurrence of Brønsted sites able to protonate ammonia at 373 K. They estimate that about 80% of the ammonia adsorbed on a silica-rich sample was held on Brønsted sites.

On ZrO_2 both ammonia and pyridine are adsorbed mainly on Lewis sites at 423 K, as demonstrated spectroscopically by Hertl (43); a very small population of Brønsted sites able to protonate ammonia and pyridine was found. However, PyH^+ ions that do not form at 373 K on ZrO_2 were observed at 473 K (44). This observation confirms indirectly the expectation that an increase in temperature causes an increase in acidity of surface hydroxyls.

Miller *et al.* (5, 15) used pyridine adsorption at 423 K to calculate the fraction of Brønsted sites on the TS and ZS samples characterized here by PADs. Their results are reproduced in Table 1 as the ratio (Brønsted sites)/(Brønsted sites + Lewis sites). By multiplying fractional Brønsted acidity by the total acid site density (measured by ammonia TPD) we estimate total Brønsted site densities for the ZS-0.65 and ZS-2.68 samples as 1.7 and 3.5 μmol m^{-2} respectively. Note that these figures are in reasonable agreement with the *total* number of sites able to dissociate protons within the pH window of potentiometric titration (1.95 μmol m^{-1} and 2.55 μmol m^{-2}).

The conclusion is that the information obtained from pK spectra of pure oxides and mixed oxide catalysts is compatible with other data reported about the character of Brønsted acid sites on these materials. Our analysis offers both a qualitative and quantitative measure of Brønsted acidity that could be related to the catalytic activity for butene isomerization at 423 K.

It is largely accepted that the concentration and chemical reactivity of the surface hydroxyls carried by metal oxides can be correlated with the coordination of the underlying surface ions. This principle, coupled with the assumptions that surface —O and —OH groups at the oxide/solution interface are the only sites for proton binding and that all proton transfer involves the first layer of strongly adsorbed water, defines the background needed for a closer look at the pK spectra of the solid samples. The information to be obtained from PADs of the wet oxide surface will later

be used to assess the number, strength, and, possibly, nature of catalytic sites at the pseudo-dry surface.

Proton Affinity Spectra of Parent Oxides

Silica. Two types of oxygen-containing surface groups (monodentate and bidentate) occur on silica surfaces. The bidentate (siloxane) group $(\equiv Si-)_2-O$ is such a weak base that it cannot be protonated within the normal pH range and should be considered inert (17, 18). Also, binding of a second proton to the single coordinated group (silanol) is not usually observed and the charging behavior is dominated by their dissociation in high pH solutions:

$$\equiv Si-OH \Leftrightarrow \equiv Si-O^- + H^+.$$

Surface silanol groups may occur isolated or may form pairs separated by a siloxane bridge. On rehydration (and in high pH solutions) the following reaction should also be considered (45):

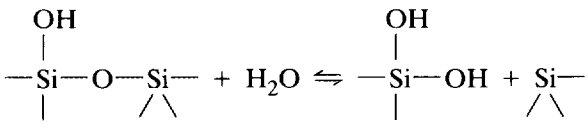

which creates more silanol groups on the surface and represents a first step toward dissolution in alkaline solutions. According to Boehm (46) and Sears (47) all surface silanol groups are neutralized below pH 9. At higher pH, opening of siloxane bonds and dissociation of silanols thus formed lead to a maximum of negative charge at about pH 10.5–10.6; on further addition of alkali, silicate ions ($H_3SiO_4^-$) are formed in solution (46).

In Fig. 5 the PAD for silica shows a flat region below pH 7 which corresponds to the known inertness of silica in neutral solutions. Above pH 7, where proton dissociation begins (Fig. 1), the pK spectrum shows ionization of silanol groups ($pK_{1(S)} = 8.0$) followed by the start of intense proton release due to breaking of siloxane groups above pH 9 followed by silanol dissociation.

Our value for the ionization constant of surface silanol groups ($pK_{1(S)} = 8.0$) is in agreement with the spectroscopically determined value (48) (pK = 7.2 ± 0.2) and the value predicted theoretically by the multisite proton adsorption model (log K = 7.5) (17, 18, 49). The surface density of sites calculated from the distribution shown in Fig. 4 is 1.4 μmol m^{-2} for silanol active at pH 8 and above. The value for siloxane is uncertain (about 2.8 μmol m^{-2}). The result of Bolt (50), for the density of negative charge at pH 10, is 3 μmol m^{-2}.

Titania. We show in Fig. 5 the PADs determined for two titania polymorphs; the result of their Gaussian analysis is shown in Fig. 8. For rutile, three proton equilibria, with $pK_{1(R)} = 5.6$ (0.29 μmol m^{-2}), $pK_{2(R)} = 6.9$ (0.89 μmol m^{-2}), and $pK_{3(R)} = 9.2$ (1.72 μmol m^{-2}) were considered. For anatase the picture is more complex and the following three groups of peaks were identified: an asymmetric peak in the acidic range (0.49 μmol m^{-2}), which was decomposed into two components with $pK_{1(A)} = 4.4$ and $pK_{2(A)} = 5.4$; a broad peak in the neutral range (0.67 μmol m^{-2}) with $pK_{3(A)} = 6.9$; and an asymmetric peak in the basic range (1.42 μmol m^{-2}) with components at $pK_{4(A)} = 8.8$ and $pK_{5(A)} = 9.7$.

A comparison with literature data is difficult. Although Boehm (51) suggested the presence on anatase of two different types of surface hydroxyls, reported experimental results mostly assumed a simple ionization scheme and perfectly amphoteric hydroxyls. Only recently the recognition of the fact that the charge at the titania–solution interface is determined by reactive groups which involve single and double coordinated oxygen atoms led to more realistic estimations. Based on the multisite proton-binding model, Hiemstra *et al.* (17, 18) predicted the following values of proton affinity constants on rutile surface:

$$(\equiv Ti-)_2-O^{-2/3} + H^+ \Leftrightarrow (\equiv Ti-)_2-OH^{+1/3}, \quad \log K_1 = 5.3$$
$$\equiv Ti-OH^{-1/3} + H^+ \Leftrightarrow \equiv Ti-OH_2^{+2/3}, \quad \log K_2 = 6.3,$$

which almost coincide with our values for $pK_{1(R)}$ and $pK_{2(R)}$. For anatase, Ludwig and Schindler (52) reported very recently three experimental values of one-step proton-binding constants: log K_1 = 5.40 (monodentate hydroxo-groups), log K_2 = 7.75 (bidentate oxo-groups), and log K_3 = 9.46 (monodentate oxo-groups). Although the assignment of the proton binding sites differs from that of Hiemstra *et al.* for rutile, two of the experimental values found for anatase are in excellent agreement with our estimation for $pK_{2(A)}$ and $pK_{5(A)}$ while the third represents the average of our $pK_{3(A)}$ and $pK_{4(A)}$.

Rutile and anatase structures are composed of the same basic units (distorted TiO_6 octahedra) but with different packing. As a consequence, in rutile there is one, and in anatase there are two oxygen-to-oxygen separations that are shorter than those predicted by simple anion–anion contact (53). Because of this we expect stronger basicity of the corresponding anion positions, which eventually results in a more complex distribution of affinity constants for real surfaces of rutile and, also, anatase. It is possible that the arrangement of terminal ions in the hydroxylated surface may differ from that of the stoichiometric crystal cleavage plane, as suggested by Jones and Hockey (54) in their infrared studies on rutile. They proposed that two distinct types of monodentate hydroxyls and two positions for hydrogen-bonded water should be assumed.

Zirconia. The PAD of pure zirconium oxide (Figs. 5 and 8) shows three major peaks: one, asymmetric

(0.36 μmol m^{-2}), with components at $pK_{1(Z)}$ = 4.5 and $pK_{2(Z)}$ = 5.4, and two, symmetric, at $pK_{3(Z)}$ = 6.7 (0.31 μmol m^{-2}) and $pK_{4(Z)}$ = 9.6 (0.29 μmol m^{-2}).

Literature information on surface charge at the zirconium dioxide–water interface is scarce. Using the classical double-layer approach, Janusz (55) reported pK values in the range of 1.5–1.8 and 6.7–7.8, depending on the calculation method used. While the first one is out of the range of accurate determination, the second coincides with our $pK_{3(Z)}$.

The experimental proof for the occurrence of several types of surface hydroxyls on zirconia polymorphs came from IR studies (43). The tetragonal ZrO_2 phase, which is formed upon calcination at 773 K of pure zirconia aerogels (11, 27) has a distorted fluorite-like structure (53) in which the octahedron of oxygen atoms around each Zr atom is composed of four first-order neighbors at 2.00 Å and four second-order neighbors at 2.47 Å. The most stable structures at the hydrated (001) surface of tetragonal zirconia were described in a recent ab initio study by Orlando *et al.* (56). On the basis of their results we propose the following equilibria with constants calculated with the multisite proton-binding model (17):

$$(\equiv Zr^{I}-)_2-OH^0 + H^+ \Leftrightarrow (\equiv Zr^{I}-)_2-OH_2^{+1}, \quad \log K_1 \approx 4.2$$

$$(\equiv Zr^{II}-)_2-OH^0 + H^+ \Leftrightarrow (\equiv Zr^{II}-)_2-OH_2^{+1}, \quad \log K_2 \approx 6.1$$

$$\equiv Zr^{II}-OH^{-1/2} + H^+ \Leftrightarrow \equiv Zr^{II}-OH_2^{+1/2}, \quad \log K_3 \approx 9.2.$$

To estimate the values of proton affinities corresponding to the above equilibria, we used the Zr–O distances calculated by Orlando *et al.* (56) for first-order (Zr^{I}) and second order (Zr^{II}) neighbors. The agreement with the experimental values (Table 2) could only be obtained with the additional assumption that the positive charge of Zr^{4+} ions was unevenly shared by monodentate and bidentate hydroxyls. This was tantamount to assuming different values for the effective bond valence of monodentate (0.6) and bidentate (0.4) hydroxyls instead of a unique value of 0.5 that results by dividing the ionic charge of Zr^{4+} by its coordination number in the ZrO_2 lattice (v = Z/CN = 4/8). Although such an assumption could be justified for a bulky cation like Zr^{4+}, the need to use it shows a weak point of the calculation procedure based only on the electrostatic bond valence principle (17–19).

Proton Affinity Spectra of Mixed Oxide Catalysts

Titania–silica. The PADs of TS samples (Fig. 4) have in common several characteristics:

- A peak with pK in the range of 4.5–5.8. It is reminiscent of bidentate hydroxyls of the titania component since similar peaks were found for both rutile and anatase (pK 4.4–5.6);
- A broad, symmetrical peak that shifts from pK 6.3 (TS-5) to pK 8–8.6 for silica-rich samples. This is the *only peak* whose population could be correlated with the activity for butene isomerization (Fig. 9);
- A peak that shifts from pK 9.1 (TS-5) to pK 10.5–10.8 and grows sharper and larger at higher silica content. It is assigned to silanol and siloxane groups from the silica component.

Miller *et al.* (5) have found on samples from the same preparation batch that the activity for butene isomerization goes through a maximum in the titania-rich region. They proposed, in line with Liu *et al.* (4), that the source of Brønsted acidity and of catalytic properties are

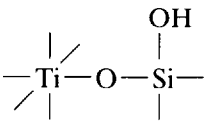

linkages where the Brønsted acidity of the silanolic hydroxyl is strengthened by the charge imbalance created between octahedral Ti and tetrahedral Si (57). Observing that anatase exhibits a broad peak at pK 6.9 (seen at pK 6.3 on TS-5) and an asymmetric peak around pK 9, one might propose an alternate explanation that localizes the acidic hydroxyl over a titanium surface ion.

Zirconia–silica. At constant ZrO_2:SiO_2 molar ratio, the differences between pK spectra of ZS samples were so subtle that they could only be resolved and quantified after decomposition of PADs into a sum of Gaussians.

- The first two peaks (pK 4.2–4.9 and pK 6.4–6.5) have an equivalent in the first and second peaks of pure zirconia. *Only the second component* of catalysts' PADs could be quantitatively related with catalytic activity for butene isomerization (Fig. 9).
- Two other peaks were resolved at pK 8.1–8.5 and pK 9.5–10.0; a third one was discerned close to pH 11, but could not be accurately analyzed because of the distortions caused by water buffering at that pH. Surface sites active in this pH domain may be located either on SiO_2 (silanols, pK $\approx$ 8.0) or on ZrO_2 (monodentate hydroxyls, pK $\approx$ 9.6). The third component at pK $\approx$ 11 represents, most probably, the onset of surface dissolution.

The acidity (and catalytic activity) is conferred to ZS catalysts by the charge imbalance associated with hetero (Zr–O–Si)-linkages. At constant 1:1 composition, the charge imbalance is constant and so is the pK observed in PADs. The effect of varying the prehydrolysis ratio is observed mainly on the location of silicon atoms, as explained by Miller and Ko (15). At high prehydrolysis

ratios more Si atoms are available to participate in hetero-linkages, accounting for the increased surface density of sites with pK $\approx$ 6.5 and the higher catalytic activity. The effect is so subtle that it cannot be obtained from a superficial examination of raw potentiometric data (Fig. 3). Only calculating PADs and their subsequent decomposition with Gaussians offered the grounds for the above proposals.

As a final word, let us mention that the above results demonstrate that both the *quantity* (abundance on catalyst surface) and the *quality* (acid strength or pK) of Brønsted sites are important for overall catalytic performance. The effect of quantity was illustrated by the ZS series, where systematic variations of the prehydrolysis ratio resulted in a better mixing of the components and created a larger number of active sites. The effect of quality is observed by comparing TS with ZS catalysts. The higher acid strength of Brønsted sites on ZS samples (pK $\approx$ 6.5) probably causes higher activity per site (turnover frequency) in the acid-catalyzed isomerization of 1-butene.

CONCLUSIONS

We have shown that the experimental measurement of proton affinity distribution at the oxide–aqueous solution interface gives reliable information, both qualitative and quantitative, on the ability of surface oxo- and hydroxo-groups for proton binding or proton release. Since the pK spectrum of the interface is a crystallochemical property, correlations with the local microstructure (atomic scale) and the charge imbalance that may affect acid–base properties are both meaningful and desirable.

For catalysts active in reactions demanding only weak Brønsted acid sites (such as double-bond isomerization of 1-butene), the pK spectrum of the wet oxide surface offers a means for the identification and quantification of those surface sites that may act as specific proton donors under the pseudo-dry conditions of catalytic tests. A linear correlation was found between specific reaction rates and the density of a surface site of a particular acid strength (or in a particular microstructural configuration) affording the possibility for counting of active sites and computation of turnover frequencies.

We have characterized two different series of mixed oxide catalysts in which the catalytic performance varied with either composition (titania–silica) or preparation parameters at constant composition (zirconia–silica). The general conclusion is that both quantity and quality of acid Brønsted sites affect the overall catalytic performance.

ACKNOWLEDGMENTS

Financial support for this work came from the Department of Energy, Division of Chemical Sciences, Office of Basic Energy Research, under Grant No. DE-FG02-92ER14268 (to J.A.S.) and Grant No. DE-FG02-93ER14345 (to E.I.K.). One of us (V.T.P.) acknowledges his support from NSF Grant No. CHE 9319593.

REFERENCES

1. Kung, H. H., "Transition Metal Oxides: Surface Chemistry and Catalysis," Elsevier, Amsterdam, 1989.
2. Ko, E. I., Chen, J.-P., and Weissman, J. G., *J. Catal.* **105,** 511 (1987).
3. Nakabayashi, H., *Bull. Chem. Soc. Jpn.* **65,** 914 (1992).
4. Liu, Z., Tabora, J., and Davis, R. J., *J. Catal.* **149,** 117 (1994).
5. Miller, J. B., Johnston, S. T., and Ko, E. I., *J. Catal.* **150,** 311 (1994).
6. Itoh, K., Hattori, H., and Tanabe, M., *J. Catal.* **35,** 225 (1974).
7. Sohn, J. R., and Jang, H. J., *J. Catal.* **136,** 267 (1992).
8. P. Jacobs, *in* "Characterization of Heterogeneous Catalysts" (F. Delanny, Ed.), p. 367. Dekker, New York, 1984.
9. Makarov, A. D., Boreskov, G. K., and Dzis'ko, V. A., *Kinet. Katal.* **2,** 84 (1961).
10. Soled, S., and McVicker, G. B., *Catal. Today* **14,** 189 (1992).
11. Miller, J. B., Rankin, S. E., and Ko, E. I., *J. Catal.* **148,** 673 (1994).
12. Bosman, H. J. M., Kruissink, E. C., van der Spoel, J., and van der Brink, F., *J. Catal.* **148,** 660 (1994).
13. Marquez-Alvarez, C., Fierro, J. L. G., Guerrero-Ruiz, A., and Rodriguez-Ramos, I., *J. Colloid Interface Sci.* **159,** 454 (1993).
14. Navio, A., Macias, M., Colon, G., and Sanchez-Soto, P. J., *Appl. Surf.* **70/71,** 226 (1993).
15. Miller, J. B., and Ko, E. I., "Advanced Techniques in Catalyst Preparations." Preprints to ACS Meeting, Anaheim, 1995.
16. Nakabayashi, H., Kakuta, N., and Ueno, A., *Bull. Soc. Chem. Jpn.* **64,** 2428 (1991).
17. Hiemstra, T., van Riemsdijk, W. H., and Bolt, G. H., *J. Colloid Interface Sci.* **133,** 91 (1989).
18. Hiemstra, T., de Wit, J. C. M., and van Riemsdijk, W. H., *J. Colloid Interface Sci.* **133,** 105 (1989).
19. Bleam, W., *J. Colloid Interface Sci.* **159,** 312 (1993).
20. Contescu, C., Jagiello, J., and Scwharz, J. A., *Langmuir* **9,** 1754 (1993).
21. Contescu, C., Hu, J., and Schwarz, J. A., *J. Chem. Soc. Faraday Trans.* **89,** 4091 (1993).
22. Contescu, C., Contescu, A., and Schwarz, J. A., *J. Phys. Chem.* **98,** 4327 (1994).
23. Contescu, C., Contescu, A., Schramm, C., Sato, R., and Scwharz, J. A., *J. Colloid Interface Sci.* **165,** 66 (1994).
24. Contescu, C., Jagiello, J., and Schwarz, J. A., *J. Phys. Chem.* **97,** 10152 (1993).
25. Bandosz, T. J., Jagiello, J., Contescu, C., and Schwarz, J. A., *Carbon* **31,** 1193 (1993).
26. Contescu, C., and Schwarz, J. A., *Appl. Catal. A: General* **118,** L5 (1994).
27. Ward, D. A., and Ko, E. I., *Chem. Mat.* **5,** 956 (1993).
28. Borkovec, M., and Koper, G. J. M., *J. Phys. Chem.* **98,** 6038 (1994).
29. Stumm, W., and Morgan, J. J., "Aquatic Chemistry," Wiley, New York, 1981.
30. Rudzinski, W., Charmas, R., and Partyka, S., *Langmuir* **7,** 354 (1991).
31. Rudzinski, W., Charmas, R., Partyka, S., Thomas, F., and Bottero, J. Y., *Langmuir* **8,** 1154 (1992).
32. Jagiello, J., *Langmuir* **10,** 2778 (1994).
33. Popovych, O., and Tomkins, R. P. T., "Nonaqueous Solution Chemistry," p. 240. Wiley, New York, 1981.
34. (a) Lin, Y., M.S. dissertation, Syracuse University, 1995. (b) Schwarz, J. A., Contescu, C., Popa, V. T., Contescu, A., and Lin, Y., submitted for publication.
35. Chang, C. C., Connor, W. C., and Kokes, R. J., *J. Phys. Chem.* **77,** 1957 (1973).
36. Miller, J. B., and Ko, E. I., submitted for publication.

37. Griffiths, D. A., and Fuerstenau, D. W., *J. Colloid Interface Sci.* **80,** 271 (1981).
38. Lyklema, J., *Chem. Ind.*, 741, (1987).
39. Finston, H. L., and Rychtman, A. C., "A New View of Current Acid–Base Theories," Wiley, New York, 1982.
40. Spitz, R., Burton, J., Barteau, M., Staley, R., and Sleight, A., *J. Phys. Chem.* **90,** 4067 (1986).
41. Hadjiivanov, K., Klissurski, D., Busca, G., and Lorenzelli, V., *J. Chem. Soc. Faraday. Trans.* **87,** 175 (1991).
42. Ingemar-Odebrand, C. U., Brandin, J. G. M., and Busca, G., *J. Catal.* **135,** 505 (1992).
43. Hertl, W., *Langmuir* **5,** 96 (1989).
44. Nakano, Y., Iizuka, T., Hattori, H., and Tanabe, K., *J. Catal.* **57,** 1 (1979).
45. Jelinek, L., and Kovats, E., *Langmuir* **10,** 4225 (1994).
46. Boehm, H. P., *in* "Advances in Catalysis," (D. D. Eley, H. Pines, and P. B. Weisz, Eds.), Vol. 16, p. 179. Academic Press, New York, 1966.
47. Sears, G. W., Jr., *Anal. Chem.* **28,** 1981 (1956).
48. Marshall, K., Ridgewell, G. L., and Rochester, C. H. *Chem. Ind. (London)* **19,** 775 (1974).
49. Hiemstra, T., and van Riemsdijk, W. H., *J. Colloid Interface Sci.* **136,** 132 (1990).
50. Bolt, G. H., *J. Phys. Chem.* **61,** 1166 (1957).
51. Boehm, H. P., *Discuss. Faraday Soc.* **52,** 264 (1971).
52. Ludwig, C., and Schindler, P. W., *J. Colloid Interface Sci.* **169,** 284 (1995).
53. Wyckoff, R. W. G., "Crystal Structures," Vol. 1. Wiley–Interscience, New York, 1963.
54. Jones, P., and Hockey, J. A., *Trans. Faraday Soc.* **67,** 2679 (1971).
55. Janusz, W., *J. Radioanal Nucl. Chem., Articles* **125,** 393 (1988).
56. Orlando, R., Pisani, C., Ruiz, E., and Sautet, P., *Surf. Sci.* **275,** 482 (1992).
57. Tanabe, K., Sumiyoshi, T., Shibata, K., Kiyoura, T., and Kitagawa, J., *Bull. Chem. Soc. Jpn.* **47,** 1064 (1974).